



Article

Bap-Independent Biofilm Formation in *Staphylococcus xylosus*

Carolin J. Schiffer ^{1,*} , Miriam Abele ², Matthias A. Ehrmann ¹ and Rudi F. Vogel ¹

¹ Lehrstuhl für Technische Mikrobiologie, Technische Universität München, 85354 Freising, Germany; matthias.ehrmann@tum.de (M.A.E.); rudi.vogel@tum.de (R.F.V.)

² Bayerisches Zentrum für Biomolekulare Massenspektrometrie (BayBioMS), 85354 Freising, Germany; m.abele@tum.de

* Correspondence: carolin.schiffer@tum.de

Abstract: The biofilm associated protein (Bap) is recognised as the essential component for biofilm formation in *Staphylococcus aureus* V329 and has been predicted as important for other species as well. Although Bap orthologs are also present in most *S. xylosus* strains, their contribution to biofilm formation has not yet been demonstrated. In this study, different experimental approaches were used to elucidate the effect of Bap on biofilm formation in *S. xylosus* and the motif structure of two biofilm-forming *S. xylosus* strains TMW 2.1023 and TMW 2.1523 was compared to Bap of *S. aureus* V329. We found that despite an identical structural arrangement into four regions, Bap from *S. xylosus* differs in key factors to Bap of *S. aureus*, i.e., isoelectric point of aggregation prone Region B, protein homology and type of repeats. Disruption of *bap* had no effect on aggregation behavior of selected *S. xylosus* strains and biofilm formation was unaffected (TMW 2.1023) or at best slightly reduced under neutral conditions (TMW 2.1523). Further, we could not observe any typical characteristics of a *S. aureus* Bap-positive phenotype such as functional impairment by calcium addition and rough colony morphology on congo red agar (CRA). A dominating role of Bap in cell aggregation and biofilm formation as reported mainly for *S. aureus* V329 was not observed. In contrast, this work demonstrates that functions of *S. aureus* Bap cannot easily be extrapolated to *S. xylosus* Bap, which appears as non-essential for biofilm formation in this species. We therefore suggest that biofilm formation in *S. xylosus* follows different and multifactorial mechanisms.

Keywords: *Staphylococcus xylosus*; knockout; Bap; biofilm; aggregation



Citation: Schiffer, C.J.; Abele, M.; Ehrmann, M.A.; Vogel, R.F. Bap-Independent Biofilm Formation in *Staphylococcus xylosus*. *Microorganisms* **2021**, *9*, 2610. <https://doi.org/10.3390/microorganisms9122610>

Academic Editor: Edward Fox

Received: 30 November 2021

Accepted: 15 December 2021

Published: 17 December 2021

Publisher's Note: MDPI stays neutral with regard to jurisdictional claims in published maps and institutional affiliations.



Copyright: © 2021 by the authors. Licensee MDPI, Basel, Switzerland. This article is an open access article distributed under the terms and conditions of the Creative Commons Attribution (CC BY) license (<https://creativecommons.org/licenses/by/4.0/>).

1. Introduction

Staphylococcus (S.) xylosus is a Gram-positive, coagulase-negative commensal of mammal skin with a biotechnological relevance, as it is commonly used as a starter organism for raw sausage fermentation [1]. For persistence in such environments, surface colonization and the formation of biofilms are anticipated as important traits. Biofilm formation is a common property of many bacteria and describes a state where cells are embedded in an extracellular matrix, mainly consisting of exopolysaccharides, proteins and extracellular DNA [2]. Biofilm matrix composition can vary and is dependent on species-specific mechanisms as well as environmental conditions [3]. If biofilms are of a mainly proteinaceous nature, surface proteins play a prominent role in primary adhesion and biofilm maturation as they can either interact with surface structures on adjacent cells or form amyloid structures that promote cellular aggregation [4]. Known surface proteins influencing proteinaceous biofilm matrix assembly include fibronectin binding proteins (FnBPs), *Staphylococcus aureus* surface protein G (SasG) and the biofilm associated protein (Bap) [5,6]. Bap is a high molecular weight surface protein, which was first described by Cucarella et al. [7]. Bap and its homologues have been shown to mediate multicellular aggregation as well as biofilm formation in several organisms, such as staphylococci and enterococci [8,9]. In *S. aureus*, V329 Bap is extensively studied, and it has been demonstrated that its functionality is based on self-assembly of N-terminal peptides of the protein into amyloid fibers

under acidic conditions [9]. Furthermore, Bap-mediated biofilm formation is influenced by calcium ions in the environment, as they prevent amyloid assembly of Bap-derived peptides and subsequent intercellular aggregation [10]. Other than in the well-studied *S. aureus* V329, Bap function has only been molecularly characterized by the construction of knockout mutants in *S. epidermidis* C533 [11]. Studies addressing *bap* of biofilm-positive *S. xylosus* strains have been focusing solely on presence/absence of the gene analysed by PCR/hybridization approaches so far [11,12]. Thus, the actual function of the protein in *S. xylosus* has not been verified experimentally yet.

In a previous study, we demonstrated a strain-specific behavior in biofilm formation among different *S. xylosus* strains depending on environmental conditions as well as their individual genomic settings with respect to additional biofilm-related genes [13]. The fact that a strain in which *bap* is naturally defective displayed a biofilm negative phenotype led us to suggest an essential role of Bap in biofilm formation of *S. xylosus*. In order to test this hypothesis and to ensure that any impact of other genomic determinants is excluded, we generated isogenic *bap* knockout mutants of biofilm positive strains. Furthermore, we investigated whether *S. xylosus* and its *bap* mutants show typical phenotypic characteristics and differences, as they have been reported in Bap-positive *S. aureus* strains and its respective *bap* mutants.

2. Materials and Methods

2.1. Bacterial Strains and Culture Conditions

S. xylosus TMW 2.1023 and TMW 2.1523 are both biofilm-positive strains, isolated from raw fermented sausages [13]. *Escherichia (E.) coli* DC10B is a cytosine methyltransferase-negative derivative, often used in transformation experiments to evade type IV restriction modification systems [14].

E. coli DC10B was cultured in Lysogeny Broth (LB, tryptone 10 g/L, yeast extract 5 g/L, NaCl 5 g/L) 37 °C. Staphylococcal strains were cultured at 28 or 37 °C in Trypticase soy broth (TSB, casein peptone 15 g/L, soy peptone 15 g/L, yeast extract 3 g/L) supplemented with either no glucose (TSB_N) or 1% glucose (TSB⁺), brain heart infusion (BHI) broth, or basic medium (BM, 1% peptone, 0.5% yeast extract, 0.5% NaCl, 0.1% Glucose, 0.1% K₂HPO₄). For transformation experiments, 20 µg/mL (*E. coli*) or 10 µg/mL (*S. xylosus*) of chloramphenicol (CarlRoth, Karlsruhe, Germany) were added when necessary.

2.2. DNA Manipulations and Bacterial Transformation: Mutagenesis of the Chromosomal Bap Gene by Allelic Exchange

For inactivation of *bap* in *S. xylosus*, regions up—and downstream of the sequence to be deleted were amplified using primers *bap*1F (5'-ACTCACTATAGGGCGAATTGGAGCTGTTATCAGCAGCTGCTAAG-3'), *bap*2R (5'-GTATATTGCGACACAATGTAAAGTATATCAG-3'), *bap*3F (5'-CTTTACATTGTGTGCGCAATATACAGCTAG-3') and *bap*4R (5'-GCTTGA TATCGAATTCCTGCAGCATCTATAACTTTAGCTG-3'). To be able to use the same primer set for both *S. xylosus* strains (TMW 2.1023, TMW 2.1523), primers were chosen to map on conserved regions of the gene. PCR products were purified using a Monarch PCR and DNA cleanup kit (New England Biolabs (NEB), Ipswich, United States). Shuttle vector pIMAY*, which was kindly provided by A. Gründling (Molecular Microbiology, Imperial College London, UK) was digested with restriction enzymes *SacI* and *PstI* and PCR fragments were ligated into the vector using Gibson Assembly (NEB). The construct was transformed into *E. coli* DC10B by electroporation and successful transformants were selected on chloramphenicol plates. Sequencing, to verify correct assembly of the vector, followed. Plasmid was isolated using the Monarch plasmid DNA miniprep kit (NEB) and transformed into electrocompetent *S. xylosus* cells as described by Monk et al. [15]. Briefly, *S. xylosus* was cultured overnight in BHI and diluted to an OD₆₀₀ of 0.5 in BM the next morning. Cultures were then incubated at 37 °C and 200 rpm for another 40 min, harvested, washed twice with ice-cold water and another two times with 10% glycerol in decelerating volumes (1/10, 1/25). Finally, cells were resuspended in 1/200 volume 10% glycerol +

500 mM sucrose and directly subjected to electroporation. At least 1 µg of plasmid was transformed (0.2 cm, 2.5 kV) and cells were immediately suspended in 1 mL BHI + 200 mM sucrose. After one hour at 28 °C, cells were spread on BHI 20CM and incubated at 28 °C for two days. Colonies were picked and allelic replacement was performed as described by Schuster et al. [16]. Lastly, successful allele replacement of the chromosomal *bap* sequence as well as plasmid loss were verified by colony PCR using primers *bap1F* and *bap4R*.

2.3. Colony Morphology on CRA

Colony morphology of wildtype and mutant strains on congo red agar (CRA, 10 g/L glucose, 0.8 g/L congo red) was assessed as previously described [17]. As congo red interacts with proteins and proteinaceous structures, strains with rough colony margins were considered as Bap positive, whereas Bap negative strains usually retain smooth colony margins.

2.4. Biofilm Formation Assays

Biofilm formation was quantified in 96-well plates as described by Schiffer et al. [13]. Strains were cultured in different media (TSB_N, TSB⁺ (pH 7.2), Lac⁺ (TSB⁺ acidified with lactic acid to pH 6.0) and on different supports (hydrophobic (Sarstedt, Nürmbrecht, Germany), hydrophilic (Nunclon™ delta, Thermo scientific, Waltham, MA, USA)). The media chosen, represent the three media found in a previous study to influence biofilm formation of the selected strains the most [13]. Lactic acid was used instead of an inorganic acid, as it is a prevalent acid found in one of the habitats of the species *S. xylosus* (raw fermented sausages). To determine whether calcium influences biofilm formation, CaCl₂ was added to the wells to a final concentration of 20 mM when indicated.

2.5. Bacterial Aggregation Assay

Bacterial aggregation was determined by growing cell suspensions (OD₆₀₀ at t₀: 0.1) in test tubes for 24 h at 37 °C, 200 rpm in either TSB_N or TSB⁺. Aggregation behavior was evaluated macroscopically. To investigate whether calcium has an impact on cellular aggregation behavior, CaCl₂ was added to a concentration of 20 mM when indicated.

2.6. Growth and pH Dynamics

pH changes of *S. xylosus* strains in TSB⁺ were monitored using the icinac system (AMS Systea, Rome, Italy). Growth curves were recorded by determining the optical density over a period of 33 h in a Microplate Reader (Spectrostar^{Nano}, BMG Labtech, Ortenburg, Germany).

2.7. SDS Page of Protein Extracts

Bacteria were grown in TSB_N until early stationary phase (37 °C, 200 rpm, 12 h). Then, 5 mL of cell culture were harvested (4 °C, 5000× g), washed twice with ice-cold phosphate-buffered saline (PBS) and resuspended in 150 µL PBS + 30% [wt/vol] raffinose (SigmaAldrich, St. Louis, MI, USA). Afterwards, 7 µL lysostaphin (1 mg/mL, SigmaAldrich, St. Louis, MI, USA) and 3 µL of DNaseI (1 mg/mL, SigmaAldrich, St. Louis, MI, USA) were added and after incubation at 37 °C for 2 h, protoplasts were sedimented at 8000× g for 30 min with slow deceleration. Supernatants were stored at −20 °C until subjection to SDS-PAGE analysis (10% resolving, 4% stacking gel).

2.8. Full Proteome Analysis

For full proteome analysis of *S. xylosus* cells, 0.1% of overnight cultures were diluted in fresh Lac⁺ and incubated in Erlenmeyer flasks under agitation (planktonic, 5 mL) or statically in Nunclon™ delta surface (Thermo scientific, Waltham, MA, USA) tissue culture plates (sessile, 2 mL) for 24 h at 37 °C. Cell lysis and in-solution digest were performed with minor changes according to the SPEED protocol [18]. Shortly, 2 mL of planktonic cells were harvested, washed twice with ice-cold PBS and resuspended in 100 µL of

absolute Trifluoroacetic acid (TFA). Sessile cells were also washed twice with ice-cold PBS to remove any non-adherent cells as well as to remove as many media proteins as possible, and dissolution of adherent cells was performed by carefully resuspending the biofilm in 100 μ L (TFA). All TFA cell suspensions were neutralized to pH 8.1–8.3 by adding nine volumes of Tris (2 M, pH not adjusted). Incubation in a thermomixer for 5 min at 55 °C and 450 rpm (ThermoMixerC, Eppendorf, Hamburg, Germany) as well as short centrifugation followed. Protein concentrations were determined using Bradford assay (B6916, SigmaAldrich, St. Louis, MI, USA) according to manufacturer's instructions. Then, 15 μ g of total protein amount were reduced, alkylated (10 mM Tris-(2-carboxyethyl)-phosphine, 40 mM 2-Chloroacetamide; 5 min, 95 °C) and afterwards diluted with water (1:1). Trypsin digest was performed in an enzyme to protein ratio of 1:50 overnight at 30 °C with mild agitation (400 rpm) and then stopped with 3% Formic acid (FA). Three discs of Empore C18 (3 M, Saint Paul, Minnesota, United States) material were packed in 200 μ L pipette tips. The resulting desalting columns were conditioned (100% acetonitrile, can) and equilibrated (40% ACN/0.1% FA followed by 2% ACN/0.1% FA). Peptides were loaded, washed (2% ACN/0.1% FA) and eluted (40% ACN/0.1% FA). For the determination of expression levels of Bap in sessile versus planktonic cultures, around 250 ng peptides of three biological replicates were subjected to an Ultimate 3000 RSLCnano system coupled to a Q-Exactive HF-X mass spectrometer (Thermo Fisher Scientific, Waltham, MA, USA). All acquisition parameters were the same as described by Kolbeck et al. [19]. Proteomic analysis of the mutant strains was done in single measurements. Around 250 ng of peptides were subjected to an Ultimate 3000 RSLCnano system coupled to a Fusion Lumos Tribrid mass spectrometer (Thermo Fisher Scientific, Waltham, MA, USA). All parameters were set as described by Bechtner et al. [20].

Since TMW 2.1523 is a well biofilm former in TSB_N [13], it was chosen that planktonic as well as sessile data was sampled for this particular strain not just in Lac⁺ but also in TSB_N.

2.9. Bioinformatic and Statistical Analysis

Bioinformatic analysis and comparative genomics were performed using CLC Main Workbench 8 software (CLC bio, Aarhus, Denmark). Isoelectric point (pI) and molecular weight (MW) were computed using the respective tool from the ExPASy server (available under: https://web.expasy.org/compute_pi/, accessed on 29 November 2021), InterPro (86.0) was used to predict signal peptide, transmembrane regions and cell wall anchor and ProScan (screens against PROSITE database) was used to scan for EF-hand motifs (cut off was set to 80% protein identity). Amyloidogenic regions in protein sequences were analyzed by using the amyloid finder tools FoldAmyloid [21], Aggrescan [22], Waltz-DB 2.0 [23] and Tango [24].

Peptide identification and quantification were performed using MaxQuant (v1.6.3.4) with Andromeda⁹⁷ [25,26]. MS2 spectra were searched against the NCBI proteome database of *S. xylosum* 2.1023 and 2.1523, respectively; common contaminants were included (built-in option in MaxQuant). Trypsin/P was specified as proteolytic enzyme. Precursor tolerance was set to 4.5 ppm and fragment ion tolerance to 20 ppm. Results were adjusted to 1% false discovery rate (FDR) on peptide spectrum match level and protein level employing a target-decoy approach using reversed protein sequences. Minimal peptide length was defined as 7 amino acids; the "match-between-run" function disabled. Carbamidomethylated cysteine was set as fixed and oxidation of methionine and N-terminal protein acetylation as variable modifications. Perseus version 1.6.15.0 [27] and LFQ-Analyst [28] were used for data analysis. Missing label-free quantitation (LFQ) values were imputed from normal distribution. Significant differences in intensities between the conditions chosen, were calculated by student's t-test with α set to 0.05 FDR correction (Benjamini Hochberg method) was applied to correct *p*-values. Data are, if not otherwise indicated, presented as means \pm standard errors of the means. Student's *t*-tests were performed using Perseus Version 1.6.15.0.

3. Results

3.1. Protein Motif Structural Organization of *S. xylosus* Bap

To allow conclusions on structure-function correlations, the protein structures of *S. xylosus* and *S. aureus* Bap were compared. To get an idea of the conservation of the protein along the full sequence length, each region was aligned separately. Hereby, we stuck to the four major regions of the protein which were defined previously [7,13]. Bap of *S. xylosus* TMW 2.1023 and TMW 2.1523 share high sequence similarities, with 99.4% (Region A), 99.4% (Region B), 79.5% (Region C) and 98.4% (Region D) protein identity, respectively. Strain specific differences of *S. xylosus* Bap mainly rely on the number of C-Repeats, which have previously been shown to have no impact on the biofilm function of Bap [30]. Therefore, both *S. xylosus* sequences are referred to as Bap_{XYL} in this paragraph and compared to the sequence of the phenotypically well-characterized, Bap-positive strain *S. aureus* V329 (Bap_{AUR}).

Bap_{XYL} as well as Bap_{AUR} are both high molecular weight proteins fulfilling typical criteria of surface proteins such as a 44 amino acid (aa) long N-terminal signal sequence (YSIRK motif) as well as a C-terminal hydrophobic transmembrane segment and the LPxTG cell wall anchor motif. However, deeper sequence comparison of Bap of these two species revealed some notable differences (Table 1).

While the predicted pI of the full protein sequences is almost identical (~3.9), it is noticeably lower in Bap_{XYL} when the aggregation prone Region B (Bap_{B_{AUR}}: 4.6, Bap_{B_{XYL}}: 4.4) is considered only. Further, repeating sequence patterns differ remarkably between the proteins of both species. While Bap_{AUR} carries two large repeating sequences in region A, Bap_{A_{XYL}} contains only two short tandem repeats. Similar applies for region D repeats. Bap_{D_{AUR}} repeats are rich in serine and aspartate, while Bap_{D_{XYL}} repeats are not just shorter but also lacking these amino acids and are rather rich in glycine. Another difference is the type of repeats in the C Region of the protein described for both species. For Bap_{C_{XYL}} repeats are predicted to be ig-like domain type 6 repeats, while for Bap_{C_{AUR}} repeats are characterized as ig-like domain type 3 repeats. It is also noteworthy that Bap_{XYL} carries almost twice as many predicted EF hand binding motifs than Bap_{AUR}. However, EF hand motifs EF2 and EF3 displayed by Region B of the protein, which have been shown to have a regulating effect on the activity of the protein [10], are identical in both species.

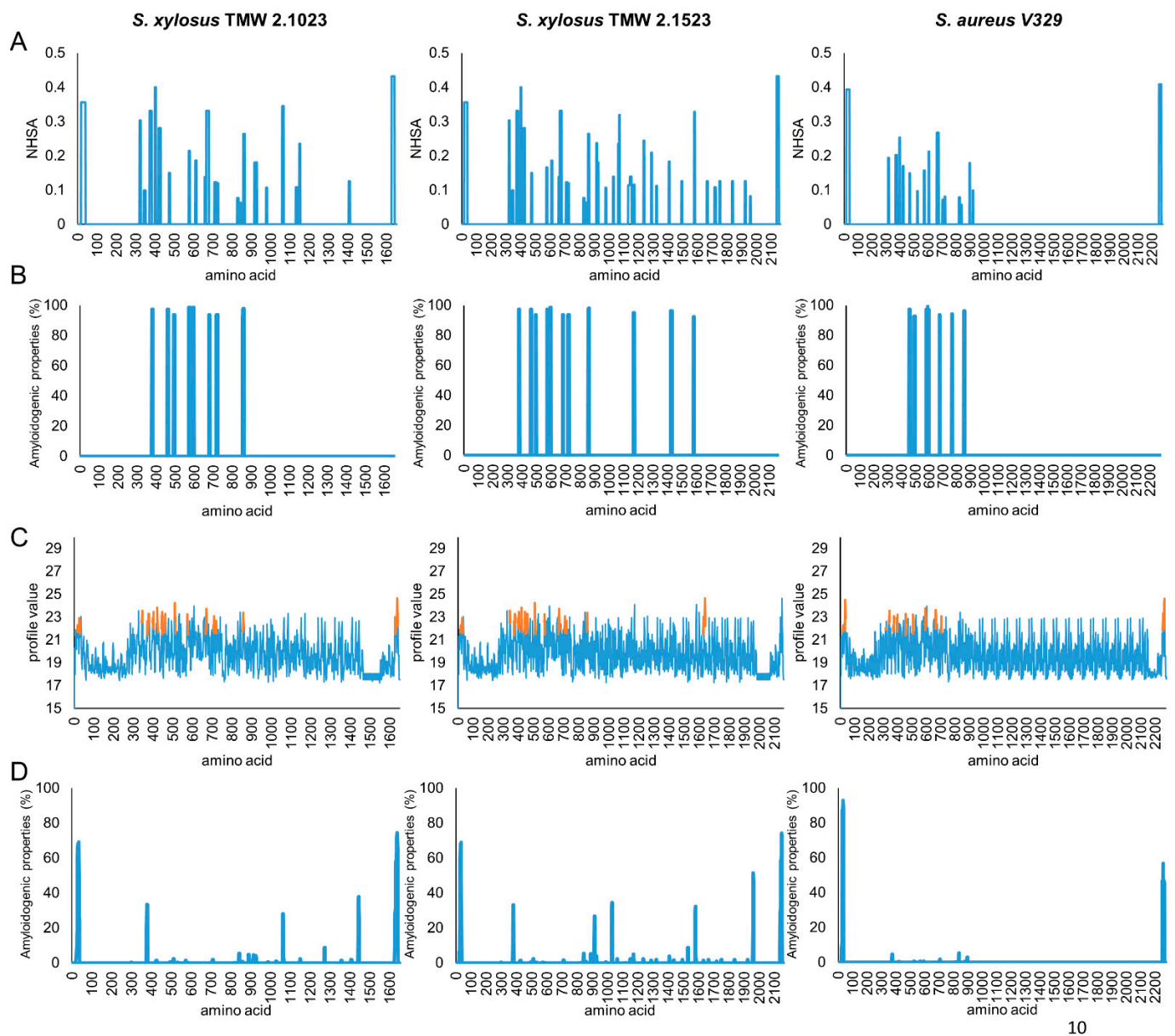
Several online tools were employed to predict amyloidogenic regions of the three protein sequences. All proteins share a region with high amyloidogenic potential, roughly between amino acid 400 and 900 (Figure 1).

However, while this region seems to be the only one with amyloidogenic potential in *S. aureus* V329, results are less conclusive for Bap_{XYL}, as, especially in TMW 2.1523, regions with amyloidogenic structural characteristics are also predicted in the C-terminal part of the protein. For Bap_{AUR}, two peptides (I: 487TVGNIISNAG₄₉₆, II: 579GIFSYS₅₈₄) are characterized as displaying significant amyloidogenic potential [9]. *S. xylosus* harbors similar peptide sequences in its Bap sequence, however, not identical (I: 490TVANILNNAG₄₉₉, II: 582GVFSYS₅₈₇). To ensure that the sequences of our selected *S. xylosus* strains are representative for the species, we compared them to a range of other *S. xylosus* bap sequences as well (see Figure S1). In this context we also included the sequence of *S. epidermidis* C533 into the alignments, as Tormo et al. [11] have previously reported a biofilm negative phenotype for this strain upon deletion of *bap*. Sequence analysis confirmed that *S. aureus* and *S. epidermidis* Bap are closely related and share high sequence homologies in all parts of the protein. *S. xylosus* bap sequences on the other hand, share high homologies among themselves, but differ from *S. aureus* and *S. epidermidis* bap genes in some functionally important parts. Namely, they lack long amino acid repeats in region A, harbor slightly different amyloidprone peptide sequences in region B, carry different types of C-repeats and are rather composed of G-rich as to SD-repeats in region D. It is further worth noting that we found a high range of truncated Bap sequences among *S. xylosus* strains, and also in biofilm positive strains ([12], e.g., *S. xylosus* C2a, accession: WP_144404228.1). This

substantiates our hypothesis that the protein is non-essential for biofilm formation by this species.

Table 1. Sequence comparison of Bap originating from *S. xyloso* TMW 2.1023, TMW 2.1523 and *S. aureus* V329. Different characteristics such as protein size, length of each region of the multidomain protein, molecular weight (MW), isoelectric point (pI) as well as number (#) of repeats and EF-hand motifs are listed.

Bap	<i>S. xyloso</i> 2.1023	<i>S. xyloso</i> 2.1523	<i>S. aureus</i> V329
Accession	JGY91_02455	JGY88_01140-45	AAK38834
Length total (aa)	1651	2161	2276
YSIRK Signal Peptide	1–44	1–44	1–44
Region A	316	316	316
Region B	458	458	458
Region C (incl. spacer)	644	1160	1321
Region D (incl LPXTG)	189	183	137
TM helix	1624–1641	2134–2151	2249–2266
MW (kDa)	173.1	224.3	238.5
pI_Bap	4.01	3.90	3.90
pI_BapB	4.41	4.39	4.61
# RepeatsA	2	2	2
sequence	TAEDN	TAEDN	AQDDDNIKEDSNTQEESTN TSSQSSEVPQTKK
# RepeatsC	7	13	14
type of C repeats	ig-like domain type 6	ig-like domain type 6	ig-like domain type 3
# RepeatsD	17	16	7
sequence	13× GTGENP, 1× GKGENP, 1× GGGENP, 1× GIGENP, 1× GTGENT	14× GTGENP, 1× GAGENP, 1× GTGENT	2× SDDNSDNGNN 1× SDDNSGNGDN 1× SDDNSDN 1× SGAGDTSN 2× SGAGDNSD
%p.identity_Xyl vs Aur	45.13	58.97	-
%p.identity_B_Xyl vs Aur	80.18	79.96	-
# EF motifs	7	7	4
seq_EF2	DYDKDGLLDYER	DYDKDGLLDYER	DYDKDGLLDYER
seq_EF3	DTDGDGKNDGDEV	DTDGDGKNDGDEV	DTDGDGKNDGDEV
%p.identity EF2_Xyl vs. Aur	100	100	-
%p.identity EF3_Xyl vs. Aur	100	100	-



10

Figure 1. Amyloidogenic structure prediction of different protein sequences from *S. xylosoy* TMW 2.1023, TMW 2.1523 and *S. aureus* V329. Prediction based on aggrescan (A), waltz (B), fold amyloid (C) and tango (D).

3.2. Mutagenesis of the Chromosomal *Bap* Gene

For mutagenesis of the chromosomal *bap* gene, 452 nt of the *bap* promoter region as well as the first 1427 nt of the *N*-terminal part of the protein in *S. xylosoy* strains TMW 2.1023 and TMW 2.1523 were deleted. To confirm successful knockout of the protein, cell extracts were at first subjected to SDS-PAGE analysis. For TMW 2.1523 a weak band was visible at the expected position for *Bap* (224 kDa) in the wildtype strain (indicated by arrow) but not in the mutant strain (Figure S2). For TMW 2.1023 no band was detectable at the position of *Bap* (173 kDa) in neither wildtype nor mutant strain.

Since visibility of *S. xylosoy* *Bap* on SDS gels was poor and inconclusive namely for strain TMW 2.1023, a high-sensitivity mass-spectrometric analysis of the full proteome was performed. *Bap* deletion was confirmed by comparing the peptide sequences mapping to *Bap* in wildtype in contrast to mutant samples. No peptide, except for one in TMW 2.1023 mutant, was found in the full proteome analysis (Table S1). This result confirmed successful knockout of *bap*.

3.3. Growth Dynamics of Wildtype and Mutant Strains

To ensure that the transformation procedure led to no growth defects as well as to investigate whether Bap deletion has an impact on the growth behavior of *S. xylosum*, growth curves in different media were recorded. Figure 2 shows the growth dynamics for both strains in TSB_N (pH 7.2), TSB⁺ (pH 7.2), Lac⁺ (pH 6) and TSB⁺-HCl (pH 6). While wildtype and mutant strains behave very similar in TSB_N and TSB⁺, curves show higher variation when the growth medium is acidified to pH 6 by either the addition of lactic acid or HCl from the very beginning. However, in general one cannot ascribe any growth deficiencies to the *bap* mutant strains.

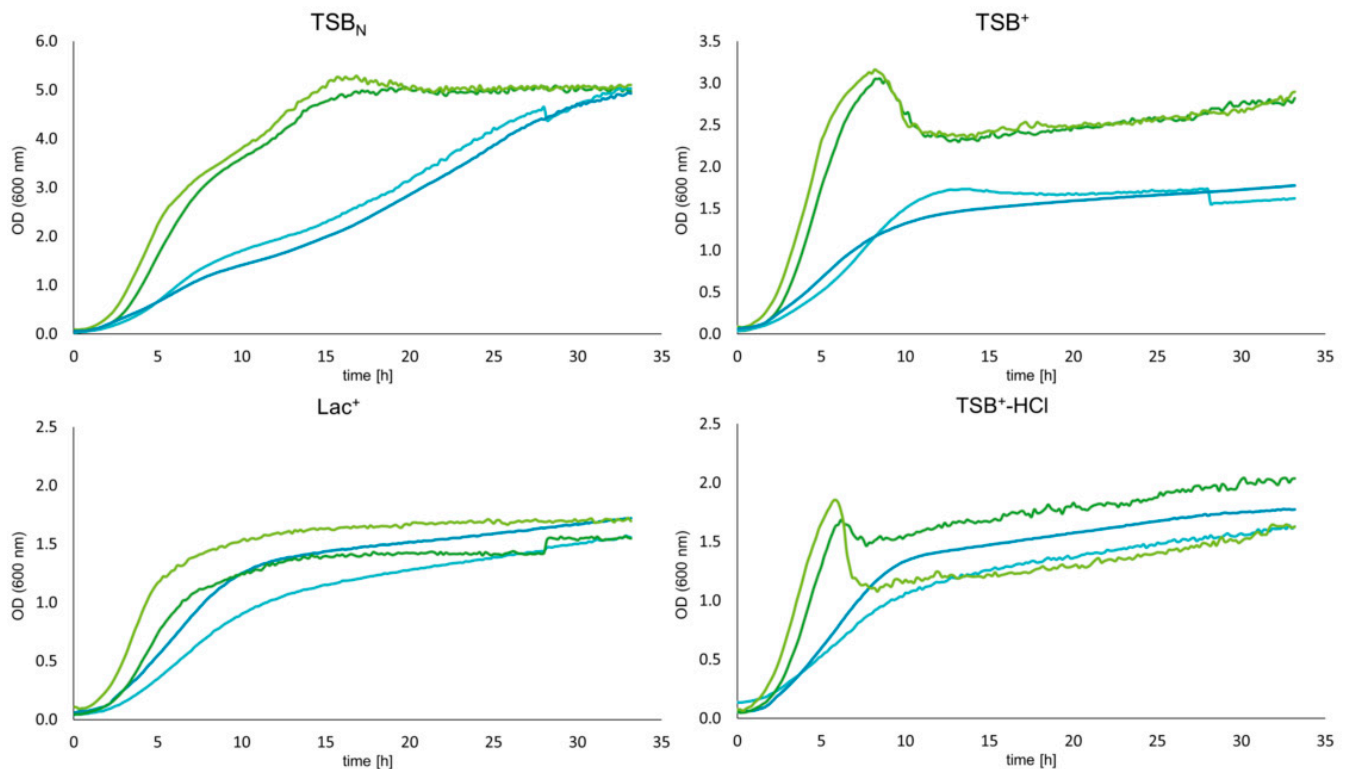


Figure 2. Growth curves of wildtype and mutant strains of *S. xylosum* TMW 2.1023 and TMW 2.1523 in different growth media (as indicated). Curves were recorded in 96-well plates in a plate reader (37 °C, aerobic conditions) every 30 min over a period of 33 h— — 023-WT, — 023-mut, — 523-WT, — 523-mut. Data are shown as mean of three biological replicates.

3.4. Biofilm Formation of Bap Wildtypes and Mutants

To determine the impact of Bap on biofilm formation of *S. xylosum*, we tested the biofilm forming capacities of two wildtype strains and their respective mutants in a 96-well plate assay. Tests were performed on hydrophilic and hydrophobic supports as well as in three different growth media that have previously been shown to promote biofilm formation to various extents in these strains [13]. The results of the biofilm assay are depicted in Figure 3. A significant reduction of biofilm formation on both supports was detectable with strain TMW 2.1523 in TSB_N only, thus in a medium where no sugar is present and therefore no pH decrease occurs upon growth. For strain TMW 2.1023, no differences in biofilm formation between wildtype and *bap* mutant strain were observed.

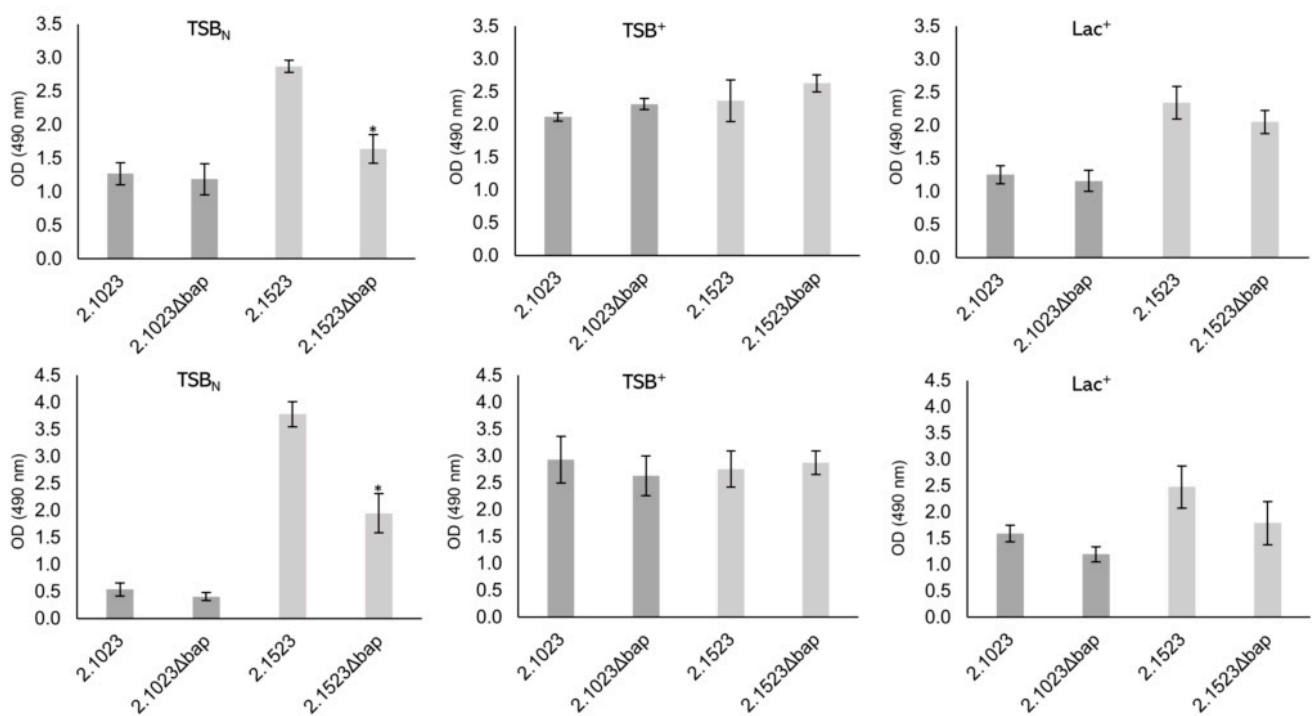


Figure 3. Biofilm formation of *S. xylosus* strains TMW 2.1023 and TMW 2.1523 and its *bap* mutants on hydrophilic (upper row) and hydrophobic (lower row) support in TSB_N, TSB⁺ and Lac⁺ (as indicated). Significant differences of means are marked by * (p -value < 0.05). Mean \pm SE.

3.5. Colony Morphology of *Bap* Wildtype and Mutant Strains on Congo Red Agar

A typical characteristic of *Bap* positive *S. aureus* strains is their rough colony morphology on congo red agar as the dye interacts with proteinaceous, fibrillar structures [31]. Loss of *Bap* causes a transformation of their rough colony morphologies to a smooth type [7]. As shown in Figure 4, we could not observe any differences in colony morphology between wildtype and mutant strains on congo red agar in *S. xylosus*. Even after a couple of days of inoculation, no switches to *Bap* positive phenotypes (rough colonies) were observable and colony margins remained smooth.



Figure 4. Colony morphology of *S. xylosus* strains on congo red agar. Bacterial overnight cultures were either streaked out for single colonies (left, middle) or applied as drops to the agar (right). Scale bar indicates 10 mm.

3.6. pH Changes of *S. xylosus* during Growth in Glucose Supplemented Media

In *S. aureus* the formation of *Bap*-based amyloid structures starts with the entry of *S. aureus* cells into stationary phase when the pH drops under pH 5 [9]. The mechanism of *Bap*-based aggregation is very sensible to pH changes, best functioning when the environment reaches pH values close to the isoelectric point of the protein. However, pH measurements over time of *S. xylosus* strains in TSB⁺ show, that *S. xylosus* is not lowering the pH below

5.0 (see Figure S3). After 24 h of pH measurement, *S. xyloso*s incubated in TSB⁺ yielded values between 5.1 ± 0.2 and 5.0 ± 0.1 for TMW 21023 and TMW 2.1523, respectively. The observed accelerated acidification of TMW 2.1023 compared to TMW 2.1523 is in concurrence with the observed, faster growth of this particular strain.

3.7. Calcium Does Not Impair Biofilm Formation of Bap Positive *S. xyloso*s Wildtype Strains

Since calcium has been described as a negative effector on biofilm formation in *S. aureus* V329 and addition of calcium to the growth medium completely abolished Bap mediated biofilm formation [10], the role of Ca²⁺ on *S. xyloso*s biofilm formation was investigated. Therefore, CaCl₂ was added to a concentration of 20 mM to the wells and biofilm formation was quantified again. As shown in Figure 5 (the respective staining results are shown in Figure S4), no biofilm-eradicating effect of calcium was found on neither of the tested supports nor in any of the tested growth media. This result leads us to hypothesize that Bap is not a major factor of *S. xyloso*s biofilm formation in these strains.

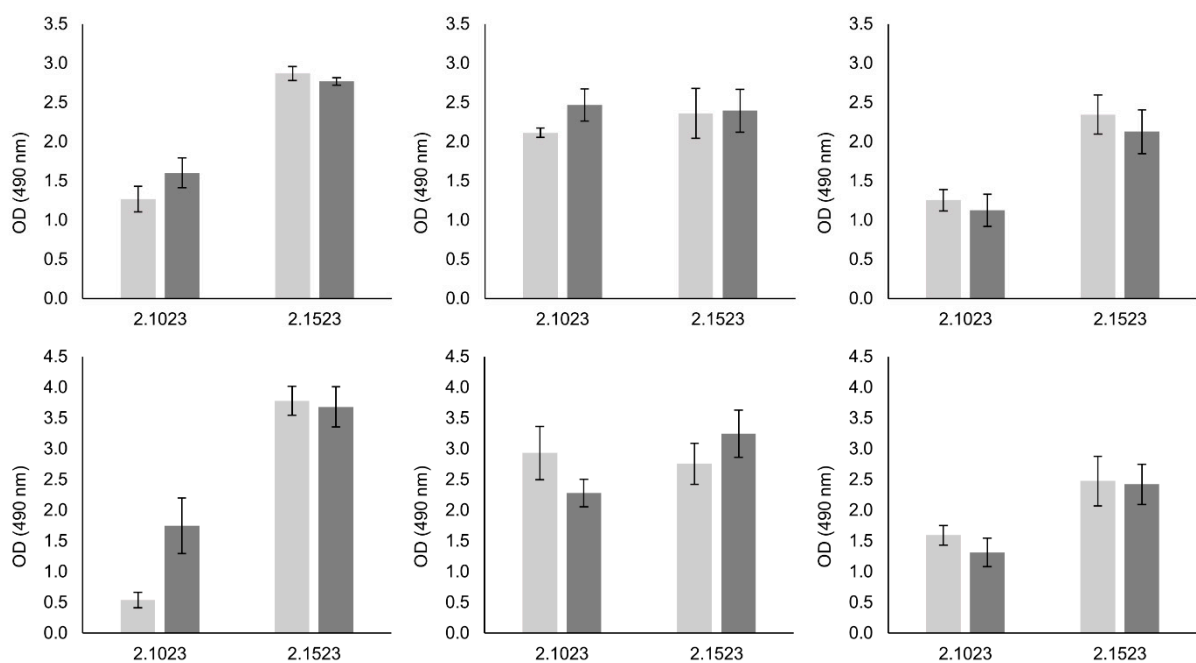


Figure 5. Effect of calcium on biofilm formation of *S. xyloso*s. Biofilm formation was quantified of *S. xyloso*s TMW 2.1023 and 2.1523 in three different media on hydrophilic (upper row) and hydrophobic (lower row) support. CaCl₂ (dark grey bars) was added to the respective growth medium to a final concentration of 20 mM.

3.8. Formation of Cell Aggregates in Wildtype and Mutant Strains

Previous studies with *S. aureus* V329 have shown that Bap is engaged in intercellular interactions, promoting aggregate formation under acidic conditions [9]. We found that *S. xyloso*s is prone to aggregation in an acidic environment, too. However, neither the absence of Bap nor addition of CaCl₂ can impair cell aggregation as it has been described for *S. aureus* V329. As shown in Figure 6, all cultures showed heavy cell clumping with cells precipitating either at the bottom of the tube or building a top layer at the air-liquid interface when incubated in TSB⁺.

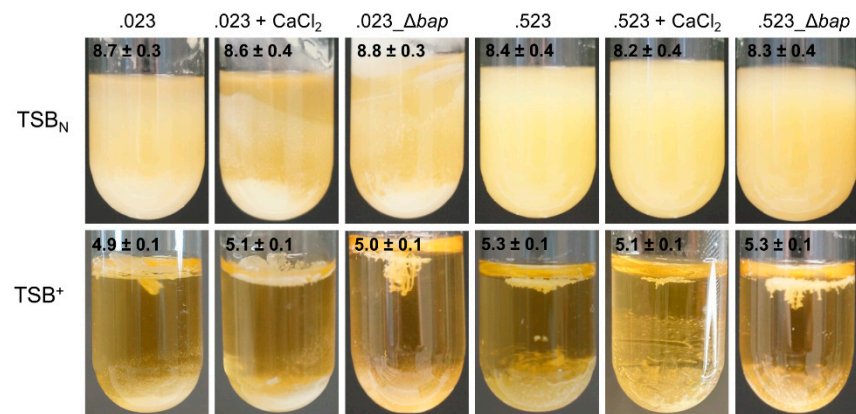


Figure 6. Aggregation behavior of *S. xylosoy* TMW 2.1023 (.023), TMW 2.1523 (.523) and the corresponding *bap* mutants grown for 24 h in TSB⁺ at 37 °C (200 rpm). Measured pH values are specified in the top left corner. CaCl₂ was added to a concentration of 20 mM when indicated.

Generally, the formation of multicellular aggregates is much weaker when strains are incubated in TSB_N, where pH remains in a neutral to basic range. Still, in neither of the media tested, any differences between wildtype and mutant strains were detectable. We further tested the aggregation and biofilm behavior of *S. xylosoy* strains when incubated in medium acidified with 1 M HCl to pH 4.5. However, no growth was detectable and thus neither aggregation nor biofilm formation could be observed. Acidification to pH 4.5 of the cells, which had been grown at neutral pH, did not lead to a change to a clumping phenotype either. Cells remained in a turbid suspension, comparable to when they were grown under neutral conditions (TSB_N).

3.9. Proteomic Analysis of Expression Levels of Bap under Planktonic versus Sessile Conditions

Since visibility of Bap on SDS page was poor, we decided to use a full proteome analysis to confirm that Bap is expressed and to monitor the expression of Bap under different conditions. Therefore, we compared the measured intensity values for Bap of both *S. xylosoy* strains when planktonic growth in Lac⁺ occurred compared to sessile growth in the same medium. Hereby, detected Bap amounts did not change significantly (TMW 2.1023) or only to a minor degree (1.15 log₂ fold, TMW 2.1523) between the two compared conditions; however, one should keep in mind that cells grown planktonically in Lac⁺ show heavy cell aggregation which is closely related to biofilm formation. On the other hand, when Bap amounts are compared in cells grown in TSB_N, the protein shows a more than fivefold reduction in biofilm stages compared to planktonic growth (Table 2, Figure S4, note: TSB_N data only available for TMW 2.1523).

Further, Bap expression is significantly higher (+2.97) when TMW 2.1523 planktonic cells are grown in TSB_N compared to Lac⁺.

In order to obtain a better understanding of whether Bap of *S. xylosoy* is a protein with a generally low abundance in the cell, Bap intensity values were not just compared between samples obtained from cells at different growth stages but also within samples. Plotting all protein intensities measured in one sample under one condition, reveals that Bap is not a highly abundant protein such as, for example, ribosomal proteins are. However, Bap expression is not remarkably low either (compare Figure S6).

Table 2. LFQ intensities determined during full proteome analysis for two different *S. xylosus* strains in two different growth media. Indicated are log₂ fold change of intensity values, adjusted (Benjamini-Hochberg method) *p*-values and whether the change in expression between the compared conditions is considered as statistically significant ($\alpha = 0.05$, True vs. False). If the log₂ fold change was <2, true is written in italics.

		Biofilm Associated Protein (Bap)		
TMW 2.1023	plankt. vs. sessile, Lac ⁺		JGY91_02455	
		log ₂ fold change	0.901	
		<i>p</i> .val (adj.)	0.158	
		significant	FALSE	
	TMW 2.1523	plankt. vs. sessile, Lac ⁺		JGY88_01140-45
			log ₂ fold change	1.15
<i>p</i> .val (adj.)			0.0189	
		significant	TRUE	
plankt. vs. sessile, TSB _N		log ₂ fold change	5.11	
		<i>p</i> .val (adj.)	0.0000231	
		significant	TRUE	
Lac ⁺ vs. TSB _N (plankt.)		log ₂ fold change	−2.97	
		<i>p</i> .val (adj.)	0.000139	
	significant	TRUE		
Lac ⁺ vs. TSB _N (sessil)	log ₂ fold change	0.981		
	<i>p</i> .val (adj.)	0.0356		
	significant	FALSE		

4. Discussion

In this study different experimental approaches were used to evaluate the impact of Bap in *S. xylosus* on its anticipated general role in biofilm formation and multicellular behavior. Therefore two *S. xylosus* wildtype strains were chosen, that have previously been shown to display different biofilm positive phenotypes [13]. After genetic and phenotypic comparison of the two strains and their isogenic *bap* mutants we found that the role of Bap in *S. xylosus* is most likely non-essential for biofilm formation, apparently strain-specific, and predictively more diverse than anticipated. Upon deletion of *bap*, a significant reduction in biofilm formation was only observed with *S. xylosus* TMW 2.1523 under neutral pH environmental conditions. It did not affect its aggregation behavior and had no effect on any of the investigated traits of *S. xylosus* TMW 2.1023. This is in contrast to studies on *S. aureus* V329 [7] and *S. epidermidis* C533 [11], which showed that disruption of *bap* led to complete abolishment of biofilm formation. We therefore conclude that, firstly, *bap* orthologs do not necessarily have the same function in other staphylococcal species as the one previously determined for single strains of *S. aureus* and *S. epidermidis* and secondly, that biofilm formation and aggregation of *S. xylosus* involves different mechanisms. This view is supported by our previous study, which revealed that different *S. xylosus* strains encode a variable set of biofilm related genes in their genomes and display a biofilm phenotype that is dependent on environmental conditions in a strain-specific manner [13]. It is also supported by the observation that *S. xylosus* C2a has been described as a strong biofilm producer [12], even though we found that Bap is truncated by a premature stop codon in region B in this strain. Given this, it appears likely that either other factors dominate biofilm formation of the species, such as eDNA, which has been named as an important component of *S. xylosus* C2a biofilm matrix [32], or that Bap does not have a predominant role in *S. xylosus* biofilm formation, due to either low expression or functional differences of the protein.

Congo red is commonly used as amyloid dye and has been shown to interact with amyloidogenic structures formed by the N-terminal part of Bap [9,31] resulting in rough colony phenotypes of Bap positive strains on CRA. Loss of Bap has subsequently been shown to transform rough colonies to colonies with smooth margins [31]. Even though *S. xylosus* strains TMW 2.1023 and TMW 2.1523 are Bap positive, no colony morphology changes in wildtype versus mutant strains could be observed. Both strains and their respective mutants displayed smooth colony margins, suggesting that in contrary to Bap positive *S. aureus* strains, (Bap based-) amyloid formation seems to be different or at least under the conditions tested, not existent in *S. xylosus*. Another factor supporting a minor role of Bap in biofilm formation of *S. xylosus* is that calcium addition (20 mM) had neither an inhibiting effect on cell aggregation in culture tubes nor on biofilm formation. In *S. aureus* V329 adding as little as 6 mM calcium to the growth medium already abolishes any kind of aggregation and biofilm formation behavior [10]. If Bap binds calcium ions with low affinity, the molten globule conformation of the protein is stabilized in a way that no subsequent assembly to amyloid structures occurs. The effect of calcium binding and stabilization is attributed to EF domains 2 and 3 in the B region of the protein. However, even though Bap_{XYL} harbors the exact same EF hand motifs in its B region as Bap_{AUR}, no aggregation/biofilm reducing effects were observed upon calcium addition. On the contrary, in some cases one could rather predict a trend towards an enhancing effect on biofilm formation especially on hydrophobic support. If and to which extent the increased number of EF hand motifs found in Bap_{XYL}, compared to Bap_{AUR}, is related to this observation remains speculative.

pH plays an important factor in Bap-mediated biofilm formation, as self-assembly of the protein into amyloid fibers occurs under acidic conditions only. When *S. aureus* V329 is incubated in medium containing glucose, pH drops below 5 as soon as stationary phase is entered, thereby approaching the pI of the aggregation prone B region of the protein, which facilitates amyloid structure formation [9]. *S. xylosus* differs in two points. First, the calculated pI of Region B of Bap_{XYL} is 4.4 compared to Bap_{AUR} 4.6, thus, considerably lower. Secondly, *S. xylosus* is not lowering the pH below 5 in medium containing glucose. Hence, even though amyloidogenic potential of Bap_{XYL} was predicted by several amyloid finders in silico, peptide self-assembly into amyloids is impeded, as a pH close to the pI of Bap_{XYL} is not reached during sugar fermentation of the organism. A final pH of 5 and not lower, after glucose fermentation by *S. xylosus*, is in consistence with our observation that *S. xylosus*, contrary to *S. aureus* [9], did not show any growth in medium with pH 4.5.

While glucose has been discussed to indirectly regulate biofilm formation of *S. aureus* [33] and acidosis related to glucose metabolism is essential for biofilm formation in Bap⁺ *S. aureus* strains [9], it is noteworthy that *S. xylosus* is a well biofilm former under neutral to basic conditions (TSB_N) and that pH decrease during growth is, in contrast to *S. aureus* V329, not necessary to induce biofilm formation. Additionally, the only reduction in biofilm formation between wildtype and mutant strain we observed was when strain TMW 2.1523 was grown under neutral conditions. Besides the already mentioned fact that the pH drop during growth of *S. xylosus* might not be low enough to induce Bap derived peptide aggregation, one could also argue that Bap might not be expressed in sufficient amounts, especially under acidic conditions, to promote formation of multicellular aggregates. This is substantiated by the results obtained from full proteome analysis which revealed a significantly higher amount of Bap_{2.1523} in neutral (TSB_N) compared to acidic (Lac⁺) medium. Moreover, even though multiple authors reported good visibility of Bap on SDS gels [7,10], *S. xylosus* Bap was poorly visible on the gel, and only a slight band was detectable for strain TMW 2.1523 when grown in TSB_N. This leads us to hypothesize that Bap_{AUR} is expressed to a higher extent than Bap_{XYL}. Whether Bap_{XYL} visibility on SDS gels is impaired by any processing that occurs, as described for Bap_{AUR} under acidic conditions [9], cannot be ruled out and should be kept in mind.

Another difference between the two species to be considered is the structural organization of the proteins. While Bap of *S. epidermidis*, *S. chromogenes*, *S. hyicus* and *S. simulans*

share almost 100% protein similarity with Bap_{AUR} [11], Bap_{XYL} and Bap_{AUR} show only around 50 (our study) to 80% [11] protein identity. Thus, different functions cannot be excluded, especially since the correlation between Bap and staphylococcal biofilm formation has mainly been studied extensively in strain *S. aureus* V329 and a function has been solely assigned to the N-terminal region of the protein so far. A large part of the protein (C-terminal part) remains bound to the cell surface, with a still unknown purpose for the cell. Lastly, small but predictively important sequence differences need to be considered, for example two short peptide sequences that have been predicted to show high amyloidogenic potential in Bap_{AUR} [9] are not conserved across the two species. Also, Bap_{AUR} Region D is rich in SD repeats and C-terminal SD repeats have previously been described to be an important structural attribute in staphylococcal surface adhesins [34,35]. Bap_{XYL} lacks any of those SD repeat rich regions.

Proteins containing a YSIRK signal peptide and an LPxTG cell anchor motif have been discussed in different contexts in the past and different functions including peptidase and hydrolase activity have been assigned to those proteins [36,37]. Furthermore, Bhp, a Bap homolog found in *S. epidermidis*, has been speculated to mediate biofilm formation at first [11]; however, disruption of *bhp* did not result in any biofilm reduced phenotypes [38]. Thus, we suggest that biofilm formation in *S. xylosus* does not necessarily require Bap, and that its dominant role in biofilm formation is currently rather restricted to strains of selected species such as *S. aureus* and *S. epidermidis* [9,11]. Our findings further suggest that conclusions on the function of Bap drawn from studies conducted with *S. aureus* V329 should be carefully applied to other organisms carrying Bap orthologs when experimental proof is lacking. Furthermore, it appears that other proteins/mechanisms must be involved in multicellular behavior and biofilm formation of *S. xylosus*.

Supplementary Materials: The following are available online at <https://www.mdpi.com/article/10.3390/microorganisms9122610/s1>, Figure S1: Bap sequence alignment of selected *S. xylosus* strains with two Bap-dependent biofilm formers: *S. epidermidis* C533 and *S. aureus* V329. Only functionally important parts of the alignment are shown. A. shows the YSIRK-Signal peptide sequence as well the difference in A-region repeat length between *S. epidermidis*/*S. aureus* and *S. xylosus*. B. shows the sequence differences between the two amyloidprone peptides (defined by Taglialegna et al. [8]) of Bap Region B (marked in yellow). C. displays the conservation across species of EF hand domains 2 and 3 (pink). D. shows the differences in D-repeats between the species. While *S. aureus* and *S. epidermidis* region D is rich in SD repeats, *S. xylosus* encodes G-rich repeats, Figure S2: Analysis of cell extract protein preparations on SDS-PAGE. Left: TMW 2.1523 wildtype (Wt) and mutant (Mt) strain, Right: TMW 2.1023 Wt and Mt. The black arrow indicates a possible location of Bap in TMW 2.1523–Wt, Figure S3: pH changes of *S. xylosus* TMW 2.1023 (grey) and 2.1523 (black) incubated in TSB⁺ aerobically at 37 °C. Changes in pH were recorded over 12 h, OD₆₀₀ at t₀ was set to 0.1. Curves display the mean of 3 biological replicates, Figure S4: Calcium (20 mM) does not impair biofilm formation of selected *S. xylosus* strains (incubated in TSB⁺, 24 h, 37 °C, stained with safranin-O), Figure S5: Boxplot of log₂ transformed LFQ intensities measured for Bap in TMW 2.1023 (A) under planktonic and sessile conditions in Lac⁺, for TMW 2.1523 (B) under planktonic and sessile conditions in Lac⁺ and TSB_N, Figure S6: Intensity based absolute quantification (iBAQ)—intensities of proteins expressed in TMW 2.1023 under planktonic (A) or sessile (B) conditions and TMW 2.1523 under planktonic Lac⁺ (A), sessile Lac⁺ (B), planktonic TSB_N (C) and sessile TSB_N (D) conditions. Bap is marked in red, highly abundant ribosomal proteins (50S) are marked in green for comparison. Table S1: Identified peptide sequences (intensity values) mapping on Bap in wildtype and mutant strains of TWW strains 2.1023 and 2.1523.

Author Contributions: C.J.S.: Conceptualization, Investigation, Methodology, Software, Visualization, Writing—Original Draft preparation; M.A.: Methodology, Software, Writing—Review and Editing; M.A.E.: Conceptualization, Supervision, Writing—Review & Editing; R.F.V.: Funding Acquisition, Project Administration, Supervision, Writing—Review & Editing. All authors have read and agreed to the published version of the manuscript.

Funding: Part of this work was funded by the German Federal Ministry for Economic Affairs and Energy via the German Federation of Industrial Research Associations (AiF) and the Forschungskreis

der Ernährungsindustrie E.V. (FEI), project AiF 19690N. M. Abele was supported by the EU Horizon 2020 grant Epic-XS.

Institutional Review Board Statement: Not applicable.

Informed Consent Statement: Not applicable.

Data Availability Statement: The proteomics raw data, MaxQuant search results and used protein sequence databases have been deposited with the ProteomeXchange Consortium via the PRIDE partner repository [29] and can be accessed using the data set identifier PXD029728. Sequencing data of TMW 2.1023 and TMW 2.1523 is accessible under JAEMUG000000000 and CP066721-CP066725, respectively.

Conflicts of Interest: The authors received research grants from the AiF, which did not influence the aims or setup of this study, and declare no conflict of interest.

References

- Leroy, S.; Vermassen, A.; Ras, G.; Talon, R. Insight into the genome of *Staphylococcus xylosum*, a ubiquitous species well adapted to meat products. *Microorganisms* **2017**, *5*, 52. [[CrossRef](#)]
- Flemming, H.-C.; Wingender, J. The biofilm matrix. *Nat. Rev. Microbiol.* **2010**, *8*, 623–633. [[CrossRef](#)] [[PubMed](#)]
- Götz, F. Staphylococcus and biofilms. *Mol. Microbiol.* **2002**, *43*, 1367–1378. [[CrossRef](#)]
- Taglialegna, A.; Lasa, I.; Valle, J. Amyloid structures as biofilm matrix scaffolds. *J. Bacteriol.* **2016**, *198*, 2579–2588. [[CrossRef](#)]
- Valle, J.; Latasa, C.; Gil, C.; Toledo-Arana, A.; Solano, C.; Penadés, J.R.; Lasa, I. Bap, a biofilm matrix protein of *Staphylococcus aureus* prevents cellular internalization through binding to GP96 host receptor. *PLoS Pathog.* **2012**, *8*, e1002843. [[CrossRef](#)]
- Speziale, P.; Pietrocola, G.; Foster, T.J.; Geoghegan, J.A. Protein-based biofilm matrices in Staphylococci. *Front. Cell. Infect. Microbiol.* **2014**, *4*, 171. [[CrossRef](#)]
- Cucarella, C.; Solano, C.; Valle, J.; Amorena, B.; Lasa, I.; Penadés, J.R. Bap, a *Staphylococcus aureus* surface protein involved in biofilm formation. *J. Bacteriol.* **2001**, *183*, 2888–2896. [[CrossRef](#)]
- Taglialegna, A.; Matilla-Cuenca, L.; Dorado-Morales, P.; Navarro, S.; Ventura, S.; Garnett, J.A.; Lasa, I.; Valle, J. The biofilm-associated surface protein Esp of *Enterococcus faecalis* forms amyloid-like fibers. *NPJ Biofilms Microbiomes* **2020**, *6*, 15. [[CrossRef](#)] [[PubMed](#)]
- Taglialegna, A.; Navarro, S.; Ventura, S.; Garnett, J.A.; Matthews, S.; Penades, J.R.; Lasa, I.; Valle, J. Staphylococcal Bap proteins build amyloid scaffold biofilm matrices in response to environmental signals. *PLoS Pathog.* **2016**, *12*, e1005711. [[CrossRef](#)]
- Arrizubieta, M.J.; Toledo-Arana, A.; Amorena, B.; Penadés, J.R.; Lasa, I. Calcium inhibits Bap-dependent multicellular behavior in *Staphylococcus aureus*. *J. Bacteriol.* **2004**, *186*, 7490–7498. [[CrossRef](#)] [[PubMed](#)]
- Tormo, M.A.; Knecht, E.; Götz, F.; Lasa, I.; Penades, J.R. Bap-dependent biofilm formation by pathogenic species of *Staphylococcus*: Evidence of horizontal gene transfer? *Microbiology* **2005**, *151*, 2465–2475. [[CrossRef](#)]
- Planchon, S.; Gaillard-Martinie, B.; Dordet-Frisoni, E.; Bellon-Fontaine, M.N.; Leroy, S.; Labadie, J.; Hébraud, M.; Talon, R. Formation of biofilm by *Staphylococcus xylosum*. *Int. J. Food Microbiol.* **2006**, *109*, 88–96. [[CrossRef](#)]
- Schiffer, C.; Hilgarth, M.; Ehrmann, M.; Vogel, R.F. Bap and cell surface hydrophobicity are important factors in *Staphylococcus xylosum* biofilm formation. *Front. Microbiol.* **2019**, *10*, 1387. [[CrossRef](#)] [[PubMed](#)]
- Monk, I.R.; Shah, I.M.; Xu, M.; Tan, M.-W.; Foster, T.J. Transforming the Untransformable: Application of Direct Transformation To Manipulate Genetically *Staphylococcus aureus* and *Staphylococcus epidermidis*. *MBio* **2012**, *3*, e00277-11. [[CrossRef](#)]
- Monk, I.R.; Stinear, T.P. From cloning to mutant in 5 days: Rapid allelic exchange in *Staphylococcus aureus*. *Access Microbiol.* **2021**, *3*, 1–7. [[CrossRef](#)]
- Schuster, C.F.; Howard, S.A.; Gründling, A. Use of the counter selectable marker PheS* for genome engineering in *Staphylococcus aureus*. *Microbiology* **2019**, *165*, 572–584. [[CrossRef](#)] [[PubMed](#)]
- Heilmann, C.; Götz, F. Further characterization of *Staphylococcus epidermidis* transposon mutants deficient in primary attachment or intercellular adhesion. *Zent. Bakteriell.* **1998**, *287*, 69–83. [[CrossRef](#)]
- Doellinger, J.; Schneider, A.; Hoeller, M.; Lasch, P. Sample Preparation by Easy Extraction and Digestion (SPEED)—A Universal, Rapid, and Detergent-free Protocol for Proteomics Based on Acid Extraction. *Mol. Cell. Proteom.* **2020**, *19*, 209–222. [[CrossRef](#)]
- Kolbeck, S.; Ludwig, C.; Meng, C.; Hilgarth, M.; Vogel, R.F. Comparative Proteomics of Meat Spoilage Bacteria Predicts Drivers for Their Coexistence on Modified Atmosphere Packaged Meat. *Front. Microbiol.* **2020**, *11*, 209. [[CrossRef](#)] [[PubMed](#)]
- Bechtner, J.; Ludwig, C.; Kiening, M.; Jakob, F.; Vogel, R.F. Living the Sweet Life: How *Liquorilactobacillus hordeii* TMW 1.1822 Changes Its Behavior in the Presence of Sucrose in Comparison to Glucose. *Foods* **2020**, *9*, 1150. [[CrossRef](#)]
- Garbuzynskiy, S.O.; Lobanov, M.Y.; Galzitskaya, O.V. FoldAmyloid: A method of prediction of amyloidogenic regions from protein sequence. *Bioinformatics* **2010**, *26*, 326–332. [[CrossRef](#)]
- De Groot, N.S.; Castillo, V.; Graña-Montes, R.; Ventura, S. AGGREGSCAN: Method, application, and perspectives for drug design. *Methods Mol. Biol.* **2012**, *819*, 199–220. [[CrossRef](#)]
- Louros, N.; Konstantoulea, K.; de Vleeschouwer, M.; Ramakers, M.; Schymkowitz, J.; Rousseau, F. WALTZ-DB 2.0: An updated database containing structural information of experimentally determined amyloid-forming peptides. *Nucleic Acids Res.* **2020**, *48*, D389–D393. [[CrossRef](#)] [[PubMed](#)]

24. Fernandez-Escamilla, A.-M.; Rousseau, F.; Schymkowitz, J.; Serrano, L. Prediction of sequence-dependent and mutational effects on the aggregation of peptides and proteins. *Nat. Biotechnol.* **2004**, *22*, 1302–1306. [[CrossRef](#)] [[PubMed](#)]
25. Cox, J.; Neuhauser, N.; Michalski, A.; Scheltema, R.A.; Olsen, J.V.; Mann, M. Andromeda: A peptide search engine integrated into the MaxQuant environment. *J. Proteome Res.* **2011**, *10*, 1794–1805. [[CrossRef](#)]
26. Tyanova, S.; Temu, T.; Cox, J. The MaxQuant computational platform for mass spectrometry-based shotgun proteomics. *Nat. Protoc.* **2016**, *11*, 2301–2319. [[CrossRef](#)]
27. Tyanova, S.; Temu, T.; Sinitcyn, P.; Carlson, A.; Hein, M.Y.; Geiger, T.; Mann, M.; Cox, J. The Perseus computational platform for comprehensive analysis of (prote)omics data. *Nat. Methods* **2016**, *13*, 731–740. [[CrossRef](#)]
28. Shah, A.D.; Goode, R.J.A.; Huang, C.; Powell, D.R.; Schittenhelm, R.B. LFQ-Analyst: An Easy-To-Use Interactive Web Platform To Analyze and Visualize Label-Free Proteomics Data Preprocessed with MaxQuant. *J. Proteome Res.* **2020**, *19*, 204–211. [[CrossRef](#)]
29. Perez-Riverol, Y.; Csordas, A.; Bai, J.; Bernal-Llinares, M.; Hewapathirana, S.; Kundu, D.J.; Inuganti, A.; Griss, J.; Mayer, G.; Eisenacher, M.; et al. The PRIDE database and related tools and resources in 2019: Improving support for quantification data. *Nucleic Acids Res.* **2019**, *47*, D442–D450. [[CrossRef](#)] [[PubMed](#)]
30. Cucarella, C.; Tormo, M.A.; Ubeda, C.; Trotonda, M.P.; Monzon, M.; Peris, C.; Amorena, B.; Lasa, I.; Penades, J.R. Role of biofilm-associated protein Bap in the pathogenesis of bovine *Staphylococcus aureus*. *Infect. Immun.* **2004**, *72*, 2177–2185. [[CrossRef](#)]
31. Tormo, M.A.; Ubeda, C.; Martí, M.; Maiques, E.; Cucarella, C.; Valle, J.; Foster, T.J.; Lasa, I.; Penadés, J.R. Phase-variable expression of the biofilm-associated protein (Bap) in *Staphylococcus aureus*. *Microbiology* **2007**, *153*, 1702–1710. [[CrossRef](#)]
32. Leroy, S.; Lebert, I.; Andant, C.; Micheau, P.; Talon, R. Investigating Extracellular DNA Release in *Staphylococcus xylosus* Biofilm In Vitro. *Microorganisms* **2021**, *9*, 2192. [[CrossRef](#)] [[PubMed](#)]
33. You, Y.; Xue, T.; Cao, L.; Zhao, L.; Sun, H.; Sun, B. *Staphylococcus aureus* glucose-induced biofilm accessory proteins, GbaAB, influence biofilm formation in a PIA-dependent manner. *Int. J. Med. Microbiol.* **2014**, *304*, 603–612. [[CrossRef](#)]
34. Bowden, M.G.; Chen, W.; Singvall, J.; Xu, Y.; Peacock, S.J.; Valtulina, V.; Speziale, P.; Höök, M. Identification and preliminary characterization of cell-wall-anchored proteins of *Staphylococcus epidermidis*. *Microbiology* **2005**, *151*, 1453–1464. [[CrossRef](#)] [[PubMed](#)]
35. McCrea, K.W.; Hartford, O.; Davis, S.; Eidhin, D.N.; Lina, G.; Speziale, P.; Foster, T.J.; Höök, M. The serine-aspartate repeat (Sdr) protein family in *Staphylococcus epidermidis*. *Microbiology* **2000**, *146*, 1535–1546. [[CrossRef](#)]
36. Bai, Q.; Ma, J.; Zhang, Z.; Zhong, X.; Pan, Z.; Zhu, Y.; Zhang, Y.; Wu, Z.; Liu, G.; Yao, H. YSIRK-G/S-directed translocation is required for *Streptococcus suis* to deliver diverse cell wall anchoring effectors contributing to bacterial pathogenicity. *Virulence* **2020**, *11*, 1539–1556. [[CrossRef](#)] [[PubMed](#)]
37. DeDent, A.; Bae, T.; Missiakas, D.M.; Schneewind, O. Signal peptides direct surface proteins to two distinct envelope locations of *Staphylococcus aureus*. *EMBO J.* **2008**, *27*, 2656–2668. [[CrossRef](#)]
38. Lasa, I.; Penadés, J.R. Bap: A family of surface proteins involved in biofilm formation. *Res. Microbiol.* **2006**, *157*, 99–107. [[CrossRef](#)] [[PubMed](#)]